Three independent methods for intermediate Jahn-Teller coupling

L. Martinelli and G. Bevilacqua
Istituto Nazionale di Fisica della Materia and Dipartimento di Fisica, Università di Pisa, Piazza Torricelli 2, 56126, Pisa, Italy

J. Rivera-Iratchet* and M. A. de Orúe
Departamento de Física, Universidad de Concepción, Casilla 160-C, Concepción, Chile

O. Mualin, E. E. Vogel,† and J. Cartes
Departamento de Física, Universidad de La Frontera, Av. Francisco Salazar 01145, Casilla 54-D, Temuco, Chile
(Received 4 January 2000)

Three different and independent methods are used to find eigenfunctions and eigenvalues for a linear Jahn-Teller Hamiltonian. They are the following: diagonalization on a Born-Oppenheimer basis developed in the adiabatic limit, diagonalization on a Glauber states basis developed in the strong-coupling limit, and construction of the eigenfunctions by means of the Lanczos method. We explore the space of interactions aiming at the intermediate-coupling limit, finding the regions of best convergence for each method. Comparison among the three methods in terms of their numerical results for energy and expected optical transitions leads to regions of total and partial agreement. Conditions for several zero-phonon lines are discussed. The dominant line is not always the threshold line and it is determined by a nontrivial balance involving all interactions. Conclusions are focused toward finding reliable methods for the different regions of the parameter space. Preparation is done for applications of this approach to explaining optical spectra of magnetic impurities in crystals under different coupling regimes.

I. INTRODUCTION

In the adiabatic approximation, the interaction between vibrations and electrons is usually ignored. However, such an approach does not always explain experiments. When vibrations and electrons are allowed to couple, the Jahn-Teller (JT) effect manifests itself in several properties.[1–6] In the present paper we want to discuss three different ways of performing numerical calculations based on independent computational algorithms, to obtain energy levels and transition probabilities for vibronic states. The presentation is kept as general as possible to allow extensions to other systems, although manifestations of the JT effect in optical properties of substitutional impurities in solids are used as a general motivation. Thus, for instance, an irregular optical spectrum with unexpected lines is an indication for the presence of such effect. We will bear in mind the case of Fe^{2+} in II-VI and III-V semiconductors of cubic symmetry, for which a substantial amount of experimental information is nowadays available[7–9] after pioneer absorption experiments performed about three decades ago.[10] Particular applications to explain zero-phonon lines in the absorption and luminescence spectra of Fe^{2+} in some II-VI and III-V compounds are underway and will be published separately, focusing on the particular properties of each family of compounds, and each compound itself.

Alternatively, the JT effect is also called vibronic coupling, since the states describing such systems extend over generalized coordinates combining vibrational and electronic spaces. The total Hamiltonian is composed of three contributions: vibrational component, electronic component plus the coupling between phonons and electrons that entangle vibrational, and electronic degrees of freedom. Beyond this point the problem resides in the way vibronic functions are found, leading to energy levels and transition probabilities. Occasionally, analytic solutions can be found for some particular couplings.[11] However, most of the time numerical solutions are the only way to approach real systems. Here we will present and apply in general three different computational methods to accomplish this task. We want to analyze and compare these methods from several points of view: mathematical procedure, operational algorithm, easiness of application, range of applicability, precision and stability of results, advantages and disadvantages of each method, and general recommendations and precautions for their use. We leave for the applications of this technique (paper under preparation) to establish the strategy to cope with the characteristics of each individual spectrum of Fe^{2+} in II-VI compounds and III-V compounds.

The three methods or techniques, which are briefly reviewed in Sec. II are the following: (a) diagonalization of the vibronic Hamiltonian in a Born-Oppenheimer basis (BO);[12–14] (b) diagonalization of the vibronic Hamiltonian in a Glauber basis (G);[15–17] (c) construction of a vibronic basis by means of a Lanczos algorithm (L).[18–23] The three procedures share the Hamiltonian, concept of vibronic functions coupled up to a certain number N of vibrational quanta, and output (energy levels and wave functions). However, each method has its own characteristic starting point and a set of appropriate operations conducted by different computer codes. So we would like to stress that results yielded by these three methods are obtained by completely independent ways. As we will see, some striking coincidences exist among the three of them or, as it is more often, between G and L, providing great confidence in the results.

Our work is numerical, so we are free to vary parameters.

Actually, the only free parameter is the so-called Jahn-Teller energy E_{JT}, which will be varied to cover weak-, intermediate-, and strong-coupling ranges. Anyhow, the treatment is done in a general way so it can be adapted to different symmetries and coupling regimes.

In Sec. II we define the Hamiltonian for a particular geometry and briefly review the three methods. In Sec. III we present results for energy differences and oscillator strengths as functions of E_{JT} for the most relevant low-temperature infrared absorptions; agreements and disagreements among the three methods are brought out. Particular limitations for each of them are pointed out. In addition, we scan the energy of the coupling phonon that is the most noticeable difference when different compounds are considered. The strong-coupling limit is addressed by considering one particularly high value of E_{JT}. In Sec. IV we draw conclusions, making recommendations for each method in different zones of the parameter space, namely for different kinds of real systems. Advantages of each method are brought out.

II. THEORY

A. Vibronic Hamiltonian

Generally speaking the total vibronic Hamiltonian can be separated into three components,

$$H = H_e + H_v + H_{JT}, \tag{1}$$

where H_e is the electronic Hamiltonian, including spin-orbit interaction ($\lambda \mathbf{S}\cdot\mathbf{L}$) and crystalline field; H_v is the vibrational Hamiltonian associated with coupling modes Q_i, of generalized momenta P_i, frequencies ω_i, and effective masses μ_i; H_{JT} is the coupling or JT Hamiltonian.

In an explicit way the vibrational component is given by

$$H_v = \sum_i \frac{\mu_i \omega_i^2}{2} Q_i^2 + \sum_i \frac{1}{2\mu_i} P_i^2, \tag{2}$$

or, in second quantized notation,

$$H_v = \sum_i \hbar\omega_i (a_i^\dagger a_i + \tfrac{1}{2}). \tag{3}$$

The coupling Hamiltonian H_{JT} is formed by a scalar product of a vector in the vibrational space $\mathbf{Q} = (Q_1, Q_2, \ldots, Q_i, \ldots)$ and a vector in the electronic coordinates $\mathbf{D} = (D_1, D_2, \ldots, D_i, \ldots)$. In terms of second quantization notation we can write

$$H_{JT} = \sum_i K_i (a_i^\dagger + a_i) D_i, \tag{4}$$

where K_i represents the coupling constant for the ith mode.

The vibrational coupling modes are the appropriate ones for each case and are decided by the local geometry. Namely, not all of the vibrational modes couple to the electronic orbitals in the same way. Usually it is only a limited number of modes that combine symmetry, abundance, and strength to be responsible for the coupling in a specific system.

Here, we will consider vibrational modes that couple strongly to the electronic orbitals of a substitutional impurity sitting at the center of a tetrahedron as often happens for crystals where covalent bonding dominates. This is usually the case of semiconductors generically designated as III-V (GaAs, GaSb, InP, InAs, etc.) and II-VI (ZnS, ZnSe, ZnTe, CdTe, etc.).

The energies of the coupling phonons must be consistent with the lattice dynamics of the host crystal. Small variations around these values are usually allowed to compensate for local symmetry breakings or frequency shifts due to the presence of impurity atoms.

We need now to be more specific with respect to the electronic orbitals to calculate measurable quantities. Let us consider magnetic impurities with incomplete d shells. Any of them splits the atomic energy levels in the presence of a crystalline field. However, all of them are still sensitive to the vibrations of the surrounding to exhibit vibronic coupling. At this point we illustrate the procedures by considering the case of d^6 shells, as in Fe^{2+} for instance, producing an ionic ground manifold of 25 states labeled as ^5D orbitals.

There are several different possibilities to continue beyond this point depending on the kind of coupling considered. By making use of the local symmetry (group T_d) we could speak of coupling to ϵ (double degenerate) or τ_2 (triply degenerate) phonons in any kind of combinations. Different authors have followed a variety of approaches.[13,24–26] In fact, one could think of any number of sets of ϵ modes plus any number of sets of τ_2 modes, which can lead to several adjustable coupling constants. However, we want to handle the minimum number of free parameters to concentrate on the merits and shortcomings of the methods. So we consider here just one set of ϵ modes, meaning only one coupling constant. Such normal coordinates are usually denoted by Q_θ and Q_ϵ, sharing a common frequency ω.

In terms of matrix representation, the five orbitals for $L = 2$ correspond to the basis functions of the irreducible representations $E + T_2$ of group T_d. On the other hand, the vibrational functions can be represented by the occupation numbers in second quantized notation $|n_\theta n_\epsilon\rangle$. We can now be more specific with respect to the scalars and matrices that appear in the Hamiltonian. The only coupling constant K can be expressed as the square root of the product of the vibrational quantum $\hbar\omega$ and the so-called Jahn-Teller energy for that mode E_{JT}. Namely,

$$K = \sqrt{\hbar\omega E_{JT}}. \tag{5}$$

The strength of the coupling is characterized by means of the Huang-Rhys factor S, defined by

$$S = \frac{E_{JT}}{\hbar\omega}. \tag{6}$$

For completeness we give next the matrix representations for the operators included in the Hamiltonian for basis functions of symmetry T_{2g} as used below,[27]

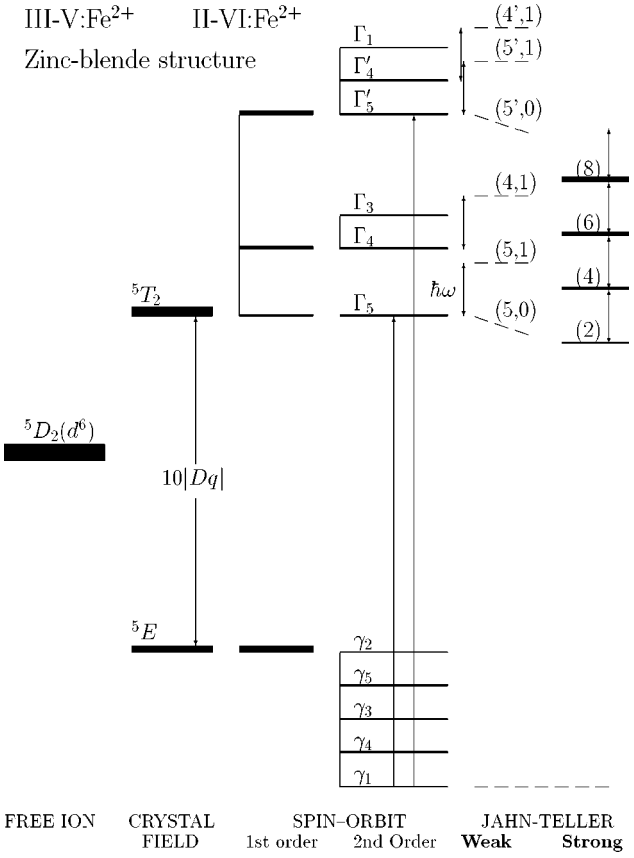

FIG. 1. Schematic of the energy levels for a magnetic impurity (Fe^{2+}) substituting for the cation in a host crystal (III-V or II-VI compounds).

$$L_x=\begin{vmatrix}0&0&0\\0&0&-i\\i&0&0\end{vmatrix},\quad L_y=\begin{vmatrix}0&0&i\\0&0&0\\-i&0&0\end{vmatrix},$$

$$L_z=\begin{vmatrix}0&-i&0\\i&0&0\\0&0&0\end{vmatrix}.$$

$$D_\theta=\begin{vmatrix}\frac{1}{2}&0&0\\0&\frac{1}{2}&0\\0&0&-1\end{vmatrix},\quad D_\epsilon=\begin{vmatrix}-\frac{\sqrt{3}}{2}&0&0\\0&\frac{\sqrt{3}}{2}&0\\0&0&0\end{vmatrix}.$$

B. Parameters

Some parameters are fixed from the knowledge of the properties of the free ion followed by crystal-field theory. We choose the data for Fe^{2+} in II-VI and III-V compounds of the zinc-blende structure. Namely $\lambda=-100$ cm^{-1} for the spin-orbit parameter and $10|Dq|\approx 2400$ cm^{-1} for the zeroth-order crystalline splitting. Splittings of successive electronic states is primarily determined by λ. This property is transferred to the energy differences among vibronic levels originating from an electronic multiplet, which are not sensitive to the exact value of $|Dq|$. In Fig. 1 we give an illustrative scheme showing electronic and vibronic levels for the example under consideration.

The energy of the coupling phonon $\hbar\omega$ is picked at fixed values up to 100 cm^{-1} that are consistent with the acoustical branches of these compounds. In particular, systematic calculations have been done at phonon energies of 35, 50, 65, and 80 cm^{-1}, aiming to characterize different zones of the parameter space.

So, the only true free parameter is the vibronic coupling itself by means of the E_{JT}. In the variation of this parameter we consider three overlapping regimes: (i) $E_{JT}<\hbar\omega$ ($S<1$) and $E_{JT}<|\lambda|$ corresponding to the weak-coupling limit; (ii) $E_{JT}\approx\hbar\omega$ and/or $E_{JT}\approx|\lambda|$ when there is competition of interactions of similar magnitude and it is called intermediate coupling; and (iii) $E_{JT}>\hbar\omega$ ($S>1$) and $E_{JT}>|\lambda|$ where the vibronic coupling dominates eventually distorting the local symmetry of the system in what is called the strong-coupling limit. Here we will scan E_{JT} between 0 and 500 cm^{-1} to run over previously defined regimes. Later on the strong-coupling limit will be studied at $E_{JT}=1000$ cm^{-1}.

C. The three methods

We describe next the three methods used to calculate vibronic coupling. However, since they have been already reported in the literature, we give just a general outline of each of them referring the interested reader to sources where a more detailed presentation is performed. Although these methods have been around for some years, there has been no attempt so far of critically comparing them under similar conditions, which is a main goal of the present paper.

D. BO method (Refs. 12–14)

The Jahn-Teller effect is assumed to be a perturbation to electrons and vibrations. Then a vibronic basis is formed by direct product of vibrational functions and electronic functions defined for the adiabatic limit (essentially at $E_{JT}\rightarrow 0$). In doing so we make use of group-theoretical properties to classify vibronic functions according to the local symmetry. There are two advantages for such an approach: vibronic states are characterized by basis functions of the corresponding irreducible representations of the appropriate point group and selection rules for optical transitions are easily observed. Such basis growths are according to the law $(N+1)(N+2)/2$, with the maximum number of vibrational quanta N. The total Hamiltonian is now diagonalized in this basis for particular values of $\hbar\omega$ chosen in advance, varying E_{JT} as described above. As E_{JT} grows, the diagonalization is achieved under more difficult conditions since H_{JT} ceases to be a perturbation to the adiabatic limit.

E. *G* method (Refs. 11,15–17)

The method of Glauber or coherent states makes use of a basis constructed in the supposedly distorted system after a strong Jahn-Teller energy has split the electronic multiplet leading to a less degenerate electronic ground state. Then a diagonalization is performed for lower values of the vibronic coupling. Full use of the point symmetry group T_d is done to improve convergence and to label wave functions. Second

quantized notation helps to speed up calculations by making use of well-known properties of Glauber states.

F. *L* recursion method (Refs. 18–23)

The use of Lanczos algorithm for Jahn-Teller systems was initiated by Muramatsu and Sakamoto,[28] followed immediately by applications by other authors.[29–33] This method is based on a progressive way of building orthonormal states for a tridiagonal representation of a given operator, such as the Hamiltonian in the present case. The initial seed state of the recursion scheme can be whatever normalized linear combination of basis states (for JT calculations a direct product of electronic and vibrational functions is suitable). In particular, for describing optical properties of JT systems it is convenient to take a dipole-carrying state[34] as the initial state of the recursion procedure (the transition of interest can further decide the particularly polarized state). Such an initial state is the linear combination of dipole-allowed states, with coefficients proportional to the matrix elements of the dipole operator. The states generated by the recursion procedure are dipole free, so the peak intensity of the lines upon diagonalization of the tridiagonal matrix is simply given by the projection modulus squared of the eigenvector on the initial chain state. In its traditional form the numerical calculations suffer from the finite arithmetic precision of computers. Instabilities in the recursion coefficients can occur and convergence is more difficult to reach for higher excited states.[35]

However, it is possible to take advantage of the loss of orthogonality of states along the Lanczos chain with the overrecursion method to find a number of lower states. The first chain state not orthogonal to some (or all) others can be considered the initial state to start a new recursion procedure. In this way, at each loss of orthogonality a new recursion chain starts. The final matrix is a *block* diagonal matrix and each block is tridiagonal. A diagonalization of such a final matrix gives us many multiple states. This is a very powerful method for telling the ''true'' (physical) eigenvalues from the ''spurious'' (numeric) eigenvalues: each true eigenvalue of the original problem is approximated often while a spurious one is not. Additionally, the spurious eigenfunction leads to an extremely weak oscillator strength and a relatively high component of the last state of the Lanczos chain. For very high excited states the modified Lanczos procedure may be required.[23]

III. RESULTS AND DISCUSSION

Now we apply the three methods varying parameters so to include the intermediate-coupling conditions which can be characterized by the criterion $0.1 \leqslant S \leqslant 10.0$ in an approximate way. Some absorption spectra of Fe^{2+} have been explained by a JT coupling close to the upper part of a previous general range. So we choose the ${}^5T_2$ multiplet originated from the ${}^5D$ ionic level as shown in Fig. 1. At very low temperatures, only absorptions originating in state γ_1 of ${}^5E$ can be expected. Selection rules for electric-dipole absorptions connect final vibronic states of total symmetry Γ_5 as illustrated in Fig. 1. They can be formed from electronic states of symmetry Γ_4 or Γ_5, coupled to phonons of symmetry ϵ, which is shown to the right of this figure. For the very-strong-coupling limit ($E_{JT} \rightarrow \infty$) vibronic levels of symmetry Γ_5 should be equally spaced at energy intervals of $\hbar\omega$ and successive degeneracies 2,4,6, . . . ,2(N+1),[16] as is shown on the extreme right of Fig. 1.

Let us recall that procedures and starting points of each method are different. BO and *G* share the diagonalization approach on the basis that is previously symmetrized to break the Hamiltonian matrix in blocks according to irreducible representations of group T_d. The orthonormal basis for BO is formed in the no-coupling limit by considering symmetrized components of the direct products ${}^5T_2 \otimes (\epsilon)^0$, ${}^5T_2 \otimes (\epsilon)^1$, ${}^5T_2 \otimes (\epsilon)^2$, . . . , ${}^5T_2 \otimes (\epsilon)^N$, with total symmetry Γ_5. (Notice that this basis is ''static'' in the sense that it does not depend on E_{JT}.) The basis for *G* requires solving the static case first, assuming a virtual displacement of the system (which depends on E_{JT}); then a nonorthogonal basis of Glauber states of symmetry Γ_5 is formed. The Lanczos procedure constructs the vibronic eigenfunctions in a recursive way starting from a seed of symmetry Γ_5 and the successive operations on it by the Hamiltonian. (This means that *L* prepares a different set of recursive eigenfunctions for each value of E_{JT}.)

For each method the functions are allowed to span a vibronic space including up to *N* vibrational quanta. Stability of the solutions was tested with respect to *N* in the sense that energy differences do not vary more than 0.5% when going from *N* to $N+1$ vibrational quanta. All results reported below (except Fig. 5) were found stable for the three methods when $N \leqslant 30$ through the entire window shown in Fig. 2. Anyhow, we have chosen to report values with $N=35$ to ensure further saturation, thus allowing the comparison of stabilized results. Both energies and relative intensities of expected absorption lines are reported.

A. Energy levels

Rather than dealing with absolute energies (E_i) we report here energy differences ($\Delta_{i1} = E_i - E_1, i = 1,2, \ldots ,7$) which is what can be read from experimental spectra. In Fig. 2 we plot six energy differences referred to as the lowest vibronic levels E_1 through E_7, using coupling modes of $\hbar\omega = 50\ \mathrm{cm}^{-1}$. The presentation in Fig. 2 is arranged in the following way: (a) bottom, results for the Born-Oppenheimer method; (b) center, results for the Glauber method; (c) top, results for the Lanczos method.

There is total agreement among the three methods from the extremely weak-coupling limit to about 200 cm^{-1} (corresponding to approximately $2|\lambda|$ or $4\hbar\omega$). At this point BO calculations begin to show differences with respect to results obtained by the other two methods that still coincide between themselves. (Agreement in terms of energy intervals can reach four digits). As E_{JT} grows, results given by BO show inconsistencies with expected tendencies toward the strong-coupling limit. At the far right of Fig. 1 we illustrated that as $E_{JT} \rightarrow \infty$ it is expected that two Γ_5 levels with a zero-phonon component should degenerate into the ground manifold. However, BO shows these levels diverging after previously coming together and eventually crossing each other ($\Delta_{21} = 0$) near $E_{JT} = 300\ \mathrm{cm}^{-1}$. Both *G* and *L* yield results that

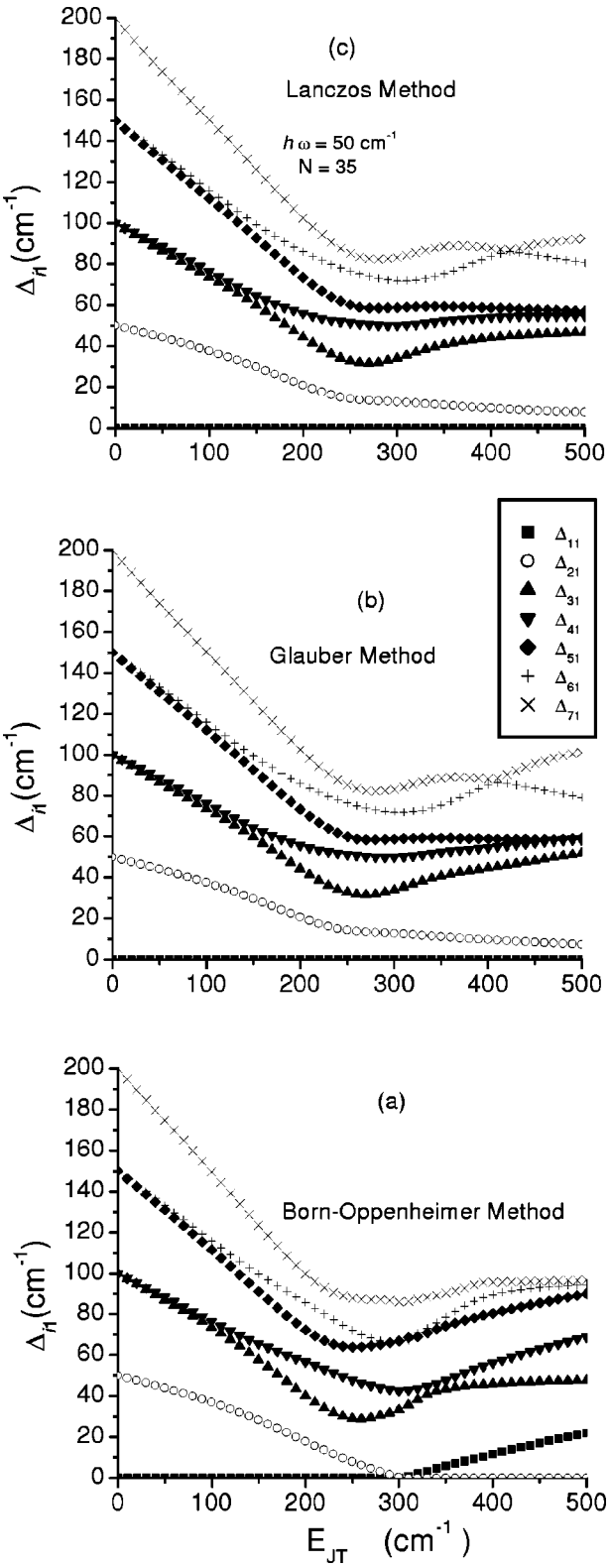

FIG. 2. Leading six energy differences ($\Delta_{i1}=E_i-E_1, i=2,\ldots,7$) of the lowest vibronic levels as functions of the Jahn-Teller energy. The energy of the coupling phonon is taken at $\hbar\omega=50$ cm^{-1}. (a) The Born-Oppenheimer method; (b) the Glauber method; (c) the Lanczos method.

are consistent with the expected behavior at the strong-coupling limit.

We prepared similar graphs to the one shown in Figs. 2(a)–2(c) considering different vibrational quanta with the general condition $\hbar\omega<|\lambda|$ (graphs not shown here). The general comments formulated for $\hbar\omega=50$ cm^{-1} hold for all of them. Additionally, we can report the following findings.

The crossing $\Delta_{21}=0$ moves very slightly toward lower values of E_{JT} as $\hbar\omega$ is diminished. So does the disagreement between BO and the other two methods. The crossing does not take place at a definite value of S. Moreover, as $\hbar\omega$ grows the value for S at the crossing decreases. We investigated how sensitive this analysis is with respect to λ by numerically varying this parameter. The results obtained by means of BO show that Δ_{21} minimizes (not always there is crossing) at slightly lower values of E_{JT} as the magnitude of the spin-orbit coupling diminishes. Always Δ_{21} diverges from there to higher values of the coupling energy in disagreement with the expected doublet. The reason for this is that eigenstates for such a strongly coupled system are far from the region of convergence of the diagonalization process based on product functions (formed at $E_{JT}=0$), such as those used by BO. In real cases λ is known, at least approximately, establishing an energy unit for comparison. Then BO can be better used for low values of E_{JT} and large values of $\hbar\omega$, which corresponds to low values of S. However, the agreement is good for $S<4$ in the case of $\hbar\omega=35$ cm^{-1}, while it is good for $S<2$ in the case of $\hbar\omega=80$ cm^{-1}. So S values cannot be used as a unique indicator for the strength of the coupling as is usually done for systems where spin-orbit coupling or other interactions do not play a significant role. Specially for intermediate coupling a full analysis involving λ, $\hbar\omega$, and E_{JT} must be done to realize the real strength of the vibronic coupling. If λ can be considered a variational parameter (which is not our case) then a full variational analysis can be done in the planes formed by S and the ratio $\lambda/(\hbar\omega)$ for successive values of the coupling vibrational quanta.

G and L agree almost exactly in the entire parameter window shown in Fig. 2. However, some slight differences begin to show for larger coupling, continuing to the right of this figure. Such disagreement is reinforced as $\hbar\omega$ takes lower values. This can be expressed as a disagreement for high values of S (certainly larger than 10). This point will be investigated in Sec. III C.

B. Absorption lines

Absolute absorption intensities are difficult to find both experimentally and theoretically since local values of temperature and shielding mask these values. So we prefer to report relative intensities F_i corresponding to transitions between the actual ground state γ_1 and the level of energy E_i as reported above ($i=1,2,\ldots,7$). Results for the leading seven absorption intensities are shown in Fig. 3 for $\hbar\omega=50$ cm^{-1}, using the same scheme as in a previous illustration (transition to the threshold line is arbitrarily normalized to unity).

The triple agreement among the methods is noteworthy under approximately 200 cm^{-1}, predicting the observation of a single absorption, precisely for the threshold line. Toward the intermediate coupling, BO predicts less lines than G and L, which still agree between themselves. Thus at 260 cm^{-1}, for instance, four lines should be clearly observed according to both G and L, while it is only three lines

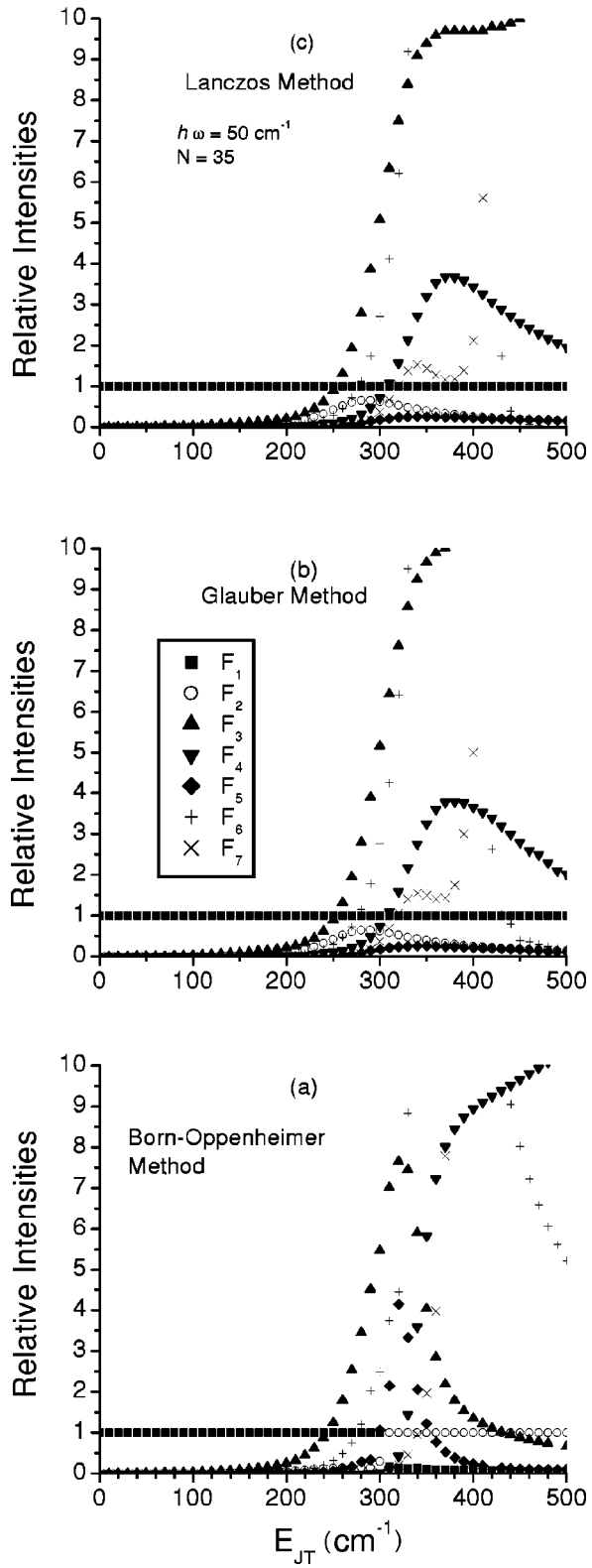

FIG. 3. Leading relative intensities for the seven energy levels involved in Fig. 1 as functions of the Jahn-Teller energy; $\hbar\omega = 50\ \mathrm{cm}^{-1}$. (a) The Born-Oppenheimer method; (b) the Glauber method; (c) the Lanczos method.

of similar intensity for BO. Even when $\hbar\omega$ is varied, BO leads to fewer intense transitions than the other two methods in the intermediate-coupling regime. Over 300 cm^{-1} BO completely disagrees with the other two methods.

Results obtained for other coupling frequencies were also plotted as in Figs. 3(a)–3(c), but they are not included here due to space limitations. Previous comments hold as $\hbar\omega$ is varied. However, as the phonon energy grows the point at which disagreement arises moves to the right. So $\hbar\omega \rightarrow 0$ marks a sector of the parameter space where BO gives energy values in disagreement with consistent and almost identical results given by G and L. Alternatively, we can say that BO is more appropriate for low values of S. From now on we continue the analysis for intermediate- and strong-coupling limits using G and L only.

As E_{JT} gets larger [right-hand side of Figs. 3(b) and 3(c)] slight disagreements between G and L are beginning to appear in a more visible way than was seen for energy differences. This is the onset of nonsaturated values for L, a point that will be further discussed when dealing with the strong-coupling regime.

In spite of the small differences in the intensities arising toward the right in Fig. 3, both G and L agree in the number of observed lines. Let us increase E_{JT} looking at the most important relative intensities within one factor of 10 [going from left to right in Fig. 3(b) or 3(c)]. Up to 200 cm^{-1} only one line should be observed (F_1). Then the absorption connecting to the third energy level (F_3) becomes the second observable line. At 220 cm^{-1}, F_2 becomes the third observable absorption line. Lets us denote such relative importance by writing the lines in an ordered way of decreasing intensities as F_1,F_3,F_2. At 250 cm^{-1} we have F_1,F_3,F_2,F_6. For 270 cm^{-1} the order is F_3,F_1,F_6,F_2,F_4. Notice that F_2 is never the dominant line for this phonon energy. We consider now the case $E_{JT}=300\ \mathrm{cm}^{-1}$ where the leading six lines would be F_3,F_6,F_1,F_4,F_2,F_7. Finally, let us notice that at 410 cm^{-1} we find F_6,F_3,F_7,F_4, an order that continues a bit beyond the right frame of Fig. 3 (this discussion applies for $\hbar\omega=50\ \mathrm{cm}^{-1}$).

Previous analysis is enough to draw two important general conclusions. (a) The number of observed lines is given by a fine tuning that relates E_{JT} to other characteristic parameters of the system. (b) The strongest absorption line (which could be mistaken as the threshold line) is not necessarily F_1 as for the weak-coupling limit; the dominant line is given by a delicate balance of parameters such as E_{JT}, λ, and $\hbar\omega$.

With the data obtained for other coupling frequencies by means of G and L we can follow the strongest absorption line in the plane $(E_{JT},\hbar\omega)$. This is done in Table I, showing that F_1 is the most intense line for weak coupling and large $\hbar\omega$ values. For intermediate coupling a serious mistake can be done if the threshold line is automatically assigned to F_1. Actually, the leading line could be extremely weak and not show up at all as happens for E_{JT} over 350 cm^{-1}. An attempt at constructing Table I (also the discussion of the previous paragraph) based on values of S failed, which suggests that sensitive transition probabilities for intermediate coupling reflect a delicate balance involving the three parameters and not only the ratio of two of them.

Usually, energies of the lines are first adjusted assuming an assignment for the threshold line based on the weak-coupling limit. In absorption, where the final states of the transition are more exposed to vibronic coupling, a different strategy should be followed. The most important feature to

TABLE I. The most intense line for different values of $\hbar\omega$ and E_{JT} (all energies in cm^{-1}). F_1 is always the most intense line for weak coupling. This property is transferred to F_3 for values of $\hbar\omega$ larger than about 40 cm^{-1} and to F_2 under it. For larger values of the coupling energy, the most intense line can be F_6 or F_7 (500+ means that this line continues to dominate beyond 500 cm^{-1}).

$\hbar\omega$	F_1	F_2	F_3	F_6	F_7
80	$0<E_{JT}<300$[a]		<400[a]	[b]	$<500+$
65	$0<E_{JT}<270$		<370	<410	$<500+$
50	$0<E_{JT}<250$		<330	<420	$<500+$
35	$0<E_{JT}<230$	<250	<280	<480	$<500+$

[a]Lanczos gives slightly lower values.

[b]Lanczos gives F_6 comparable to F_3, while for Glauber F_6 is always weaker than F_3 for this range.

be established is the relative intensities of the most important lines of the vibronic spectrum and then adjustments for the energy differences can be performed aiming to explain a particular spectrum.

One interesting implication of this analysis is that upper lines become dominant for certain ranges of the coupling. This can be expected in a general sense since coupling means mixing of zero-phonon functions with multiphonon functions. However, there is not *a priori* reasons for F_6 being dominant at intermediate coupling while F_4 and F_5 do not become dominant at any instance for the coupling under consideration. The particular behavior of F_3 is shown in Fig. 4 using G and L at four different values of $\hbar\omega$. For coupling phonons of low energies (large S values) the third line becomes very important at intermediate coupling already; in this regime results using G yield values somewhat larger than those given by L. For coupling phonons of larger energy (small values of S) F_3 should lose importance since its zero-phonon component weakens; this aspect is followed by G and L in Fig. 4. However, for $\hbar\omega=80$ cm^{-1} results using L ($N=35$) begin to show oscillations and disagreements with the expected tendency due to lack of stability. This point will be discussed for stronger coupling below.

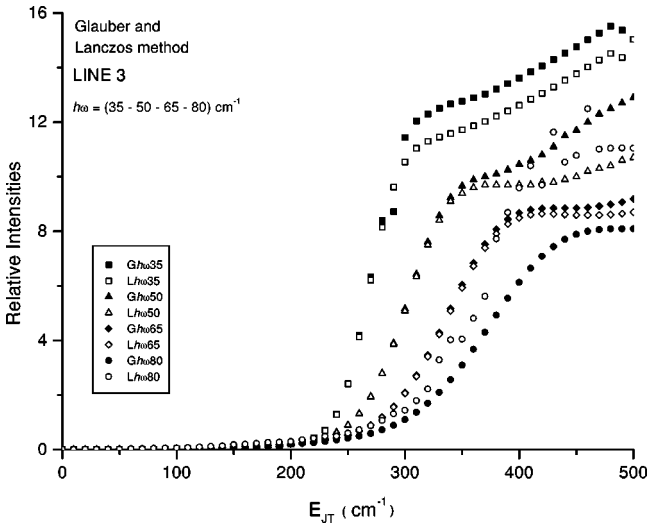

FIG. 4. Intensity of the sixth absorption line, F_3, for four values of the energy of the coupling vibration using the Glauber method and the Lanczos method ($N=35$).

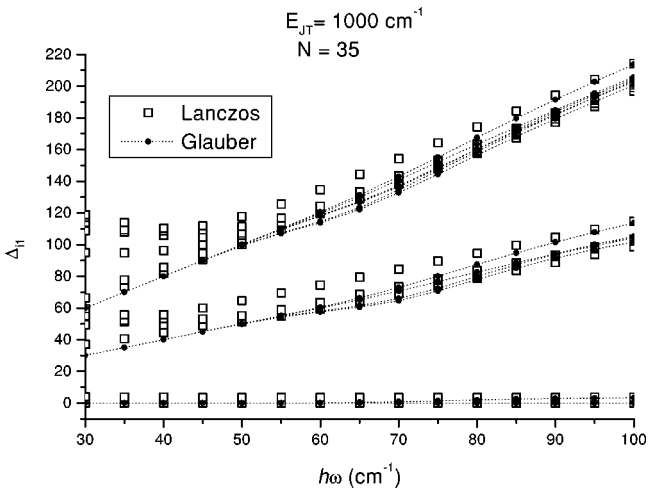

FIG. 5. Lowest 12 energy levels in the strong-coupling limit ($E_{JT}=1000$ cm^{-1}) as functions of the vibrational quantum energy ($N=35$).

It is important to realize how sensitive is the region of intermediate coupling when three characteristic energies compete (spin-orbit, vibrational quantum, and coupling energy). Analyses based only on the usual S values can be misleading here. Special strategies must be defined for applications to particular spectra. Having more than one numerical method is an advantage to do so. One main concern in numerical calculations is convergence to false attractors, then results are stable but wrong. The availability of independent methods can help to avoid and eventually reveal such behavior.

C. Strong-coupling limit

In Fig. 5 we present results for the 12 lowest-energy differences as functions of $\hbar\omega$ using G and L at the fixed value $E_{JT}=1000$ cm^{-1}, which is clearly in the strong-coupling limit ($S\gg10$ for all values of $\hbar\omega$ under consideration). Again $N=35$ but it will be a point of discussion below.

Let us recall from Fig. 1 that the expected energy level scheme is a doublet (arbitrarily at zero energy), followed by a quartet at $\hbar\omega$, then a sextet at $2\hbar\omega$. Such degeneracy is strictly obeyed by G for vibrational quanta of low energies; as $\hbar\omega$ increases upper levels begin to split but the linear dependence on the phonon energy still prevails as shown in Fig. 5. For low values of $\hbar\omega$, the present results for L yield a spread for the levels forming each multiplet instead of the expected degeneracy. Further investigation of this point showed that results given by L using $E_{JT}=1000$ cm^{-1}, with $N=35$, are not saturated. Depending on S it is necessary to increase the number of vibrational quanta to 70 (to describe accurately the lower doublet) or more if upper levels are to be reported. This observation also tells that the oscillations of results for F_3 given by L in Fig. 4 are also due to the lack of stability of the results for $N=35$.

As $\hbar\omega$ increases, the strong-coupling condition weakens which is realized by the splitting in the results obtained by G. Under these conditions, L merges with G as the phonon energy increases (and S decreases). From a different point of view, as E_{JT} decreases for a given $\hbar\omega$, L reaches stability for smaller N values, so both G and L have similar stabilities in

Figs. 2, 3, and 4. Moreover, as E_{JT} takes lower values in these figures, L reaches stability for lower values of N as compared to G. On the other hand, BO tends to stable values but they could be wrong once the initially assumed perturbation gets larger than the spin-orbit splitting.

Generally speaking, G works well for extremely strong vibronic coupling since it is tailored to work under such conditions. L converges very slowly in this limit, so very large values of N can be needed before reaching the desired convergence. As already discussed, BO fails completely in the description of the highly coupled systems, since it is designed to treat the vibronic coupling as a minor perturbation.

IV. CONCLUSIONS

The combination of the methods BO, G, and L provides a powerful tool to tackle virtually any Jahn-Teller problem to a desired order of accuracy. Their coincidental results under appropriate conditions serve as a test for the theoretical framework on which they are based, as well as the independent computer codes each method uses to calculate results.

In the weak-coupling limit, any of the three methods can be used to extract information about energy levels and wave functions. However, BO presents some advantages, which we summarize here. Energy levels are obtained directly from one diagonalization and are easy to characterize based on the symmetry present under no-coupling conditions. Convergence for energies and wave functions is attained at small values of N. Computer calculations consume little time. The second alternative in this limit is L, which might need slightly more computer time than BO to settle the matter of spurious states. This is not a serious deficiency since such nonphysical states are easily recognized. Now we can also eliminate them for comparison with results by BO. Alternatively, G can also be used in this limit as it follows from previous figures, but the convergence of this method is poor compared with any of the other two, which requires larger values of N and longer computer times.

In the intermediate-coupling limit, BO progressively finds more difficulties for properly describing excited states and even ground states. This method is definitely discouraged for E_{JT} values close to (or larger than) the splitting given by spin-orbit interaction. Here results given by G and L coincide; for low-intermediate coupling, L converges faster to stable results, while for high-intermediate coupling results given by G get stability for lower values of N. The important outcome of this analysis is that for intermediate coupling (usually the harder region to tackle in this problem) we can use now two independent methods to get reliable results to be compared with experiments.

Under conditions of intermediate coupling, the ordering of the energy levels is very sensitive to variations in the coupling. So, it is better to focus the discussion on transition probabilities to find the dominant lines first, while the assignment of the energy levels to such transitions is done afterwards. Under appropriate circumstances, the most intense absorption lines can involve any of the vibronic states. This very important observation, and the possibility of performing calculations with the most appropriate method, yield a strategy to tackle complicated manifestations of the Jahn-Teller effect in the intermediate-coupling limit. Although any of the methods (G or L) would be enough, the possibility of checking numerical results with an independent procedure will lead to reliable adjudications of the observed lines.

In the strong-coupling limit BO is completely out of range and results are unphysical. L finds progressive difficulties as the coupling becomes stronger, with the need of high values of N and large computer times to approach stable results consistent with this limit. Here is where G proves its advantages since stable physical results are readily attained with interpretations closely connected to a JT displacement, as happens for $E_{JT} \rightarrow \infty$. In such a limit, the overlap of the coherent states diminishes allowing a fast convergence.

One characteristic of the energy levels as functions of E_{JT} found by G is that they present wavelets at certain values of the variable. They have to do with the zero-phonon components originating at the Γ_5' electronic levels that should cascade all the way down to be present at the ground doublet for the strong-coupling limit. The range for which such wavelets are present can be isolated for any particular case to be further studied by means of extended calculations with larger values of N until wavelets are damped. Alternatively, L can be used as a check in such ranges to ensure agreement and reliable results.

ACKNOWLEDGMENTS

This work has been partially funded by FONDECYT (Chile) under Contract No. 1990875, the international collaboration funded by CNR'i (Italy) and Conicyt (Chile). Partial support was also due to Dirección de Investigación y Desarrollo Universidad de La Frontera and Dirección de Investigación Universidad de Concepción.

*Author deceased on May 27, 2000.
†Corresponding author: Fax: +56 45 325323; Email: evogel@ufro.cl

[1] H.A. Jahn and E. Teller, Proc. R. Soc. London, Ser. A **161**, 220 (1937).
[2] D.M. Sturge, *Solid State Physics: Advances in Research and Applications*, edited by H. Ehrenreich, F. Seitz, and D. Turnbull (Academic Press, New York, 1967), Vol. 20, p. 91.
[3] R. Englman, *The Jahn-Teller Effect in Molecules and Crystals* (Wiley-Interscience, New York, 1972).
[4] I.B. Bersuker, *The Jahn-Teller Effect and Vibronic Interactions in Quantum Chemistry* (Plenum, New York, 1984).
[5] Michael D. Kaplan and Benjamin G. Vekhter, *Cooperative Phenomena in Jahn-Teller Crystals* (Plenum Press, New York, 1995).
[6] C.C. Chancey and M.C.M. O'Brien, *The Jahn-Teller Effect in C_{60} and other Icosahedral Complexes* (Princeton University Press, Princeton, NJ, 1997).
[7] G. Rückert, K. Pressel, A. Dörnen, K. Thonke, and W. Ulrici, Phys. Rev. B **46**, 13 207 (1992) and references quoted therein.
[8] S.W. Biernacki, J. Kreissl, and H.-J. Schulz, Z. Phys. Chem. (Munich) **201**, S. 31 (1997).
[9] J. Dziesiaty, P. Peka, M.U. Lehr, A. Klimakow, S. Müller, and H.-J. Schulz, Z. Phys. Chem. (Munich) **201**, 63 (1997).
[10] G.A. Slack, F.S. Ham, and R.M. Chrenko, Phys. Rev. **152**, 376 (1966); J.M. Baranowski, J.W. Allen, and G.L. Pearson, Phys.

Rev. B **160**, 627 (1967); G.A. Slack, S. Roberts, and J.T. Vallin, *ibid.* **187**, 511 (1969); F.S. Ham and G.A. Slack, *ibid.* **4**, 777 (1971).
[11] B.R. Judd, Can. J. Phys. **52**, 999 (1974).
[12] H. Maier and U. Scherz, Phys. Status Solidi B **62**, 153 (1974).
[13] J. Rivera-Iratchet, M.A. de Orúe, and E.E. Vogel, Phys. Rev. B **34**, 3992 (1986).
[14] E.E. Vogel, O. Mualin, M.A. de Orúe, and J. Rivera-Iratchet, Phys. Rev. B **44**, 1579 (1991).
[15] B.R. Judd and E.E. Vogel, Phys. Rev. B **11**, 2427 (1975).
[16] J. Rivera-Iratchet, M.A. de Orúe, M.L Flores, and E.E. Vogel, Phys. Rev. B **47**, 10 164 (1993).
[17] E.E. Vogel, J. Rivera-Iratchet, and M.A. de Orúe, Z. Phys. Chem. (Munich) **200**, S. 227 (1997).
[18] C. Lanczos, J. Res. Natl. Bur. Stand. **45**, 250 (1950); **49**, 33 (1952); *Applied Analysis* (Prentice-Hall, Englewood Cliffs, NJ, 1956).
[19] R. Haydock, V. Heine, and M.J. Kelly, J. Phys. C **5**, 2845 (1972); **8**, 2591 (1975).
[20] D.W. Bullet, R. Haydock, V. Heine, and M.J. Kelly, in *Solid State Physics: Advances in Research and Applications*, edited by H. Ehrenreich, F. Seitz, and D. Turnbull (Academic Press, New York, 1980), Vol. 35.
[21] G. Grosso and G. Pastori Parravicini, Adv. Chem. Phys. **62**, 81 (1985); **62**, 133 (1985); see also G. Grosso and G. Pastori Parravicini, *Solid State Physics* (Academic Press, London, 2000), p. 185 and references therein.
[22] H.Q. Lin and J.E. Gubernatis, Comput. Phys. **7**, 400 (1993).
[23] G. Grosso, L. Martinelli, and G. Pastori Parravicini, Phys. Rev. B **51**, 13 033 (1995).
[24] V. Savona, F. Bassani, and S. Rodriguez, Phys. Rev. B **49**, 2408 (1994).
[25] D. Colignon and E. Kartheuser, Z. Phys. Chem. (Munich) **201**, 119 (1997).
[26] R. Hammida and A. Gerard, Z. Phys. Chem. (Munich) **201**, 127 (1997).
[27] G.F. Koster, J.O. Dimmock, R.G. Wheeler, and H. Statz, *Properties of the Thirty-Two Point Groups* (MIT University Press, Cambridge, MA, 1963).
[28] S. Muramatsu and N. Sakamoto, J. Phys. Soc. Jpn. **44**, 1640 (1978); **46**, 1273 (1979); Phys. Rev. B **17**, 868 (1978).
[29] M.C.M. O'Brien and S. Evangelou, J. Phys. C **13**, 611 (1980).
[30] E. Haller, L.S. Cederbaum, and W. Domcke, Mol. Phys. **41**, 1291 (1980).
[31] J.R. Hoffman and T.L. Estle, Phys. Rev. B **27**, 2640 (1983).
[32] L. Martinelli, G. Pastori Parravicini, and P.L. Soriani, Phys. Rev. B **32**, 4106 (1985).
[33] M.C.M. O'Brien, J. Phys. C **18**, 4963 (1985).
[34] L. Martinelli, M. Passaro, and G. Pastori Parravicini, Phys. Rev. B **39**, 13 343 (1989).
[35] J.C. Cullum and R.A, Willoughby, in *Lanczos Algorithms for Large Symmetric Eigenvalue Computations* (Birkhauser, Boston, 1985), Vols. I and II.